to be submitted to Astroparticle Physics

Observation and Simulations of the Backsplash Effects in High-Energy Gamma-Ray Telescopes Containing a Massive Calorimeter

Alexander A. Moiseev, Jonathan F. Ormes, Robert C. Hartman, Thomas E. Johnson, John W. Mitchell, and David J. Thompson

Abstract. Beam test and simulation results are presented for a study of the backsplash effects produced in a high-energy gamma-ray detector containing a massive calorimeter. An empirical formula is developed to estimate the probability (per unit area) of backsplash for different calorimeter materials and thicknesses, different incident particle energies, and at different distances from the calorimeter. The results obtained are applied to the design of Anti-Coincidence Detector (ACD) for the Large Area Telescope (LAT) on the Gamma-ray Large Area Space Telescope (GLAST).

1. Introduction. The popular scheme for high-energy gamma-ray detectors is one consisting of two main parts, the first enabling the conversion of the incident photon into an electron-positron pair and determination of their trajectories (the "tracker"), and the second measuring the energy of the photon (the "calorimeter"). A common approach is to use a calorimeter design sufficiently deep to absorb the energy of a detected incident photon, released in an electromagnetic shower developed in the calorimeter. Most of the charged particles and photons in the shower are traveling along the general direction of the incident particle, but a small fraction of them go backward, creating additional signals in the detectors in front of the calorimeter (e.g. in the tracker). Most of these signals are caused by Compton electrons, created by low attenuation photons. For incident energies above several GeV, the number of such secondary particles (denoted here as backsplash) can be significant.

A special problem appears when the detector array has an anti-coincidence shield (hereafter ACD), as do all gamma-ray telescopes to study cosmic ray gamma radiation (SAS-2 [1], COS-B [2], EGRET [3,4], Gamma-1 [5], GLAST [6] and others). The ACD is intended to respond to passage of a charged particle; its signal is used as a "veto" to reject such a background event, making possible the detection of the cosmic gamma rays, whose intensity is 4-5 orders of magnitude below that of the charged cosmic rays (protons, helium and other nuclei, electrons). In such a system the backsplash from an incident photon can create ACD signals that mimic veto signals (self-veto effect), thus causing the event to be mistakenly rejected (Figure 1). Obviously, this reduces the efficiency of gamma-ray detection, especially at the highest energies.

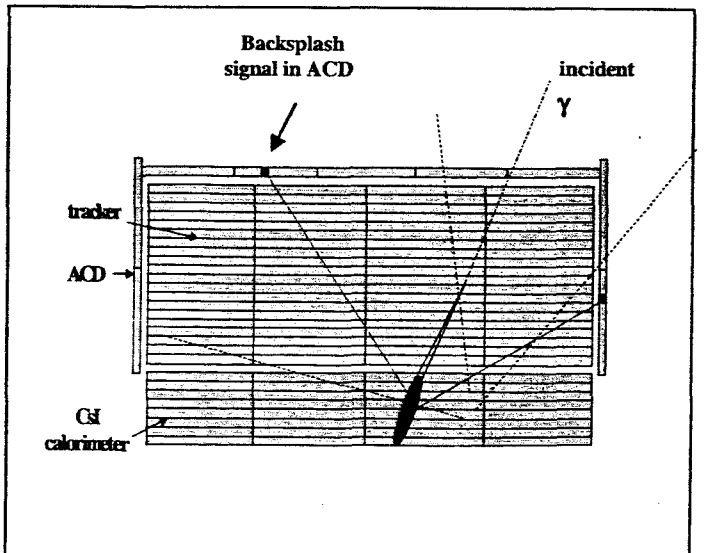

Figure 1. Backsplash in gamma-ray telescope

EGRET, the high energy gamma-ray telescope [3,4] on the Compton Gamma Ray Observatory (CGRO), experienced a gamma-ray detection efficiency degradation at an incident photon energy of 10 GeV by a factor of 2 compared to that at 1 GeV, entirely due to the self-veto effect caused by backsplash. The scientific goals of GLAST, a new high energy gamma-ray telescope under development [6], required it to be capable of detecting photons up to the range of 300-500 GeV (where the instrument will run out of statistics) without significant efficiency degradation due to backsplash. The way to suppress the backsplash effect is to segment the ACD and to consider only those veto signals that appear in the ACD segment crossed by the detected incident photon. This requires incident photon trajectory reconstruction, which is provided by the tracker. At the same time, segmented ACD becomes much more complicated from both mechanical and data acquisition points of view. Thus a deep understanding of the backsplash effect, and careful optimization of the ACD design are needed.

One approach to the design of such an instrument is the use of a simulation code to study the process of high-energy photon detection by the instrument with a heavy calorimeter, and optimize the design by minimizing the impact from backsplash. However, we have to take into account that the relevant backsplash from the calorimeter (mainly low-attenuation, several hundred keV photons) causes signals in the ACD via Compton scattering. Because the energy of the incident photon can be several hundred GeV, we must be able to track in the simulations the secondary particles in the shower down in energy by a factor of ~1,000,000. Also, optimization of the design of a complicated mechanical structure by simulations, where the code must be modified many times, is very time-consuming. At the design level, high precision in the instrument performance prediction seems to be not necessary.

The goal of the work presented in this paper, is to develop a simple qualitative method of estimating the amount of backsplash and to validate the simulation code based on the experimental data. After validation, the simulation code will be used for the detailed study of the instrument performance with greater confidence. We conducted a beam experiment to study the backsplash effect quantitatively, and then validated simulations by comparing the experimental results with the simulations.

2. Measurement of Backsplash.

2.1 Experiment goals and setup. The beam test was performed at the CERN SPS H4 beam line in July 2002. Its task was to measure pulse-height spectra of the backsplash energy deposited in the ACD, which was placed in front of a heavy calorimeter (a physical simulation). The measurements were done at different distances from the beam axis, with calorimeter simulators of different materials and different thicknesses, and for different distances between the ACD and the calorimeter. A list of beam runs performed, along with simulations run, is shown in Table 1. The result desired was the probability per unit ACD area of a signal caused by backsplash, as a function of distance from the beam axis, calorimeter material and thickness, ACD distance from the calorimeter, and threshold in the ACD. Calorimeters of lead, tin, and iron were used in the test.

E, GeV		10		20		50		100		200		250	
D,cm	Calorime-ter	Test	Sim	Test	Sim	Test	Sim	Test	Sim	Test	Sim	Test	Sim
20	Sn, $7.9X_0$					√				√	√		
30	Sn, $7.9X_0$									√			
45	Sn, $7.9X_0$	√		√		√	√	√	√	√	√	√	
	Pb, $7.9X_0$			√		√	√	√	√	√	√		
	Pb, $17X_0$					√	√	√	√	√	√		
	Pb, $30X_0$			√		√	√	√	√	√	√		
	Fe, $7.9X_0$					√	√			√	√		
60	Sn, $7.9X_0$									√			
80	Sn, $7.9X_0$					√				√	√		
Background						√		√		√		√	

Table 1. List of beam tests and simulations runs. D is the distance between the ACD and the calorimeter front plane.

A schematic of the test setup is shown in Figure 2. Although our ultimate intention was to understand backsplash from photon events, the beam test was done with an electron beam, which is much easier to produce and monitor. The difference between electron-initiated and photon-initiated showers is well understood and reproduced by shower simulation codes. The beam events were selected by the coincidence of three triggering scintillating detectors, two of which were 1cm×1cm size (T1 and T2), and the third one 10cm×10cm (T3), placed directly in front of our detecting system. The ACD was composed of 8 plastic scintillating tiles, all 1cm thick. The three closest to the beam were 8cm×24cm and the remaining five 6cm×24cm. Each tile was viewed by one Hamamatsu R647 PMT through wavelength shifting fibers embedded in grooves in the tile. The following calorimeter simulators were available:

9.5 cm thick (~$7.9X_0$) of tin (Z=50) – simulating a CsI calorimeter

14 cm thick (~$7.9X_0$) of iron (Z=26)

4.45 cm thick (~$7.9X_0$) of lead (Z=82)

9.5 cm thick (~$17X_0$) of lead

17.1 cm thick (~$30X_0$) of lead

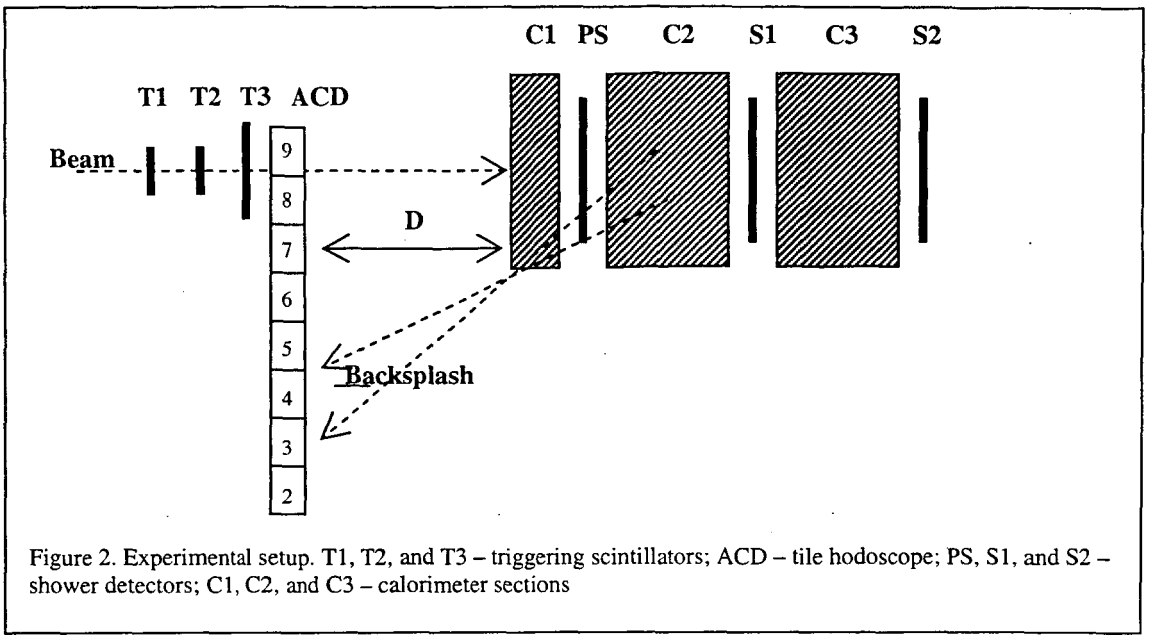

Figure 2. Experimental setup. T1, T2, and T3 – triggering scintillators; ACD – tile hodoscope; PS, S1, and S2 – shower detectors; C1, C2, and C3 – calorimeter sections

Three plastic scintillating tiles (shower detectors) are located inside the calorimeter, the first after ~$1X_0$ of calorimeter depth (PS), the second after 4-$5X_0$ (S1), and the last in the back of calorimeter (S2). They select the events that had a properly developed cascade in the calorimeter, removing hadron (mostly pion) contamination in the beam.

The ACD was placed on a remotely controlled moving table, which permitted adjustment of its position without stopping the beam and entering the beam area.

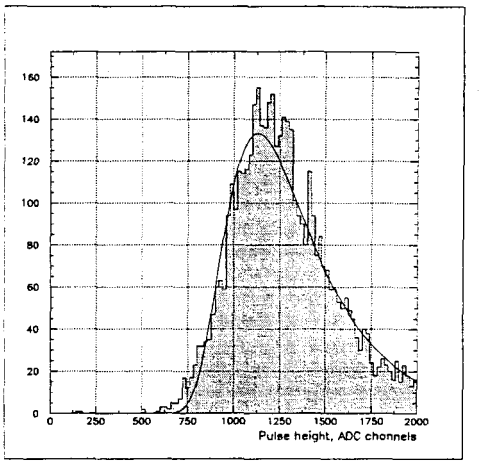

Figure 3. MIP pulse-height spectrum with peak position determined in channel 1129 (pedestal removed)

Data acquisition was provided by a CAMAC 2259 peak-sensitive LeCroy ADC, triggered by the coincidence of the three triggering scintillators. Signals digitized were from the three shower detectors and the eight ACD tiles. A typical spectrum of signals created in an ACD tile by incident charged particles (here 200 GeV protons, which were used to calibrate the system) is shown in Figure 3.

A GEANT 3.21 simulation code for the experimental setup was written, with the data analysis identical to that for the beam test experimental data. The kinetic energy cutoff for shower particles tracked in the simulations (critical to this study) was set to 100 keV.

2.2 Background. In order to measure the pulse-height spectrum in ACD tiles from backsplash events, background must be removed. The main background in this experiment is signals produced in ACD tiles by bremsstrahlung from beam electrons. The beam setup was such that the electrons were moving through ~20 meters of air between exiting the evacuated beam pipe and entering our experimental setup. Bremsstrahlung photons were created in this region, which create signals in the ACD tiles that are indistinguishable from those created by backsplash photons. In order to be able to remove that background in analysis, the pulse-height spectrum from the ACD tiles was recorded with the calorimeter removed from the beam; this was done for several different energies of incident electrons.

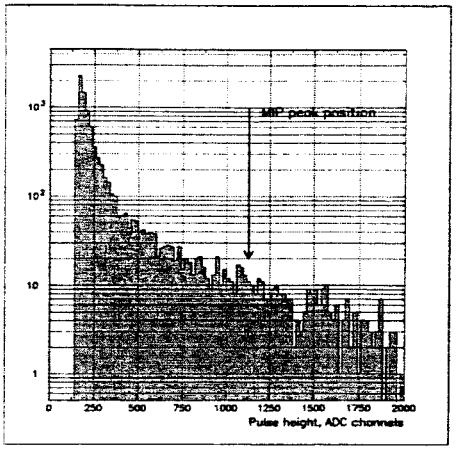

Figure 4. Typical backsplash spectrum with pedestal removed. Arrow shows where the MIP-caused peak would be (as shown in fig.3)

2.3 Data Analysis

The raw pulse-heights are converted to units of mean energy deposition in an ACD tile by normally incident minimum ionizing singly charged particles (hereafter *mip*). Special runs were performed to do pulse height calibration, with a proton beam incident on each ACD tile. An example of this spectrum is shown in Figure 3, where the peak position is determined by fitting the histogram with Landau distribution.

The data analysis procedure was the following:

1. The response of every ACD tile to a *mip* was calibrated. The *mip* peak position was determined for each tile by fitting the pulse-height histogram with a Landau distribution.
2. The backsplash spectrum (Figure 4) was developed in units of *mip* for each tile.
3. For every run the set of events that interacted in the calorimeter was selected by applying selections in the shower detectors PS, S1, and S2. This removed hadron contamination from the events to be analyzed. All further analysis steps were performed on this selected set of events.
4. For every backsplash run, the integral signal distribution in each ACD tile was produced by determining the number of events with energy deposition more than 0.1, 0.2, 0.3, 0.4, and 0.5 *mip*.
5. Background runs were treated similarly, and the measured background was subtracted from the corresponding spectrum bin in every run. The results were considered to be the backsplash-induced spectra in the ACD tiles.
6. In all results presented here (unless stated differently), the backsplash is given as the fraction of events (in percent) in which the signal in the ACD was above a given

threshold (in units of *mip*). In most figures the backsplash is given for tiles 6, 7, and 8 together, with a total area of 432 cm^2.

3. Results.

3.1. Angular distribution of backsplash. As the first step of the analysis, the angular dependence of backsplash was determined. This is important because of the necessity to check the validity of application of the results to other sizes of detectors (here, tiles). The angle at which the tile was seen from the calorimeter axis was measured between the beam axis and the line connecting the center of the calorimeter face and the corresponding tile center. The results are given in Figure 5 for five thresholds used in the analysis. Each data point represents particular tile. Hereafter the backsplash is given as the fraction of events (in percent) when the signal in an ACD tile was above a given threshold. The area of each tile was 144 cm^2 (backsplash in the larger area tiles 2, 3, and 4 was scaled to the same area). These data in Figure 5 are for a 200 GeV electron beam, taken with the tin calorimeter placed 45 cm from the ACD plane.

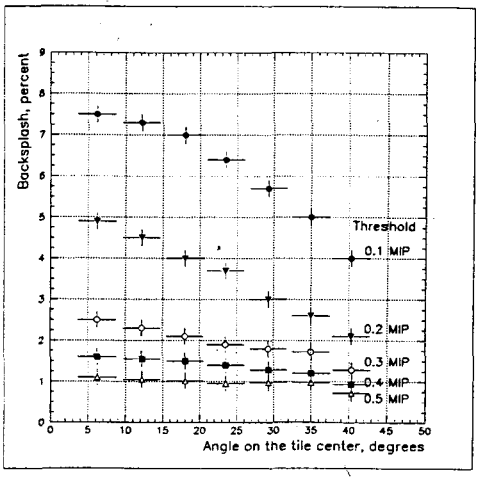

Figure 5. Angular distribution of backsplash for different thresholds. Data are for 200 GeV beam with the tin calorimeter placed at 45cm from ACD

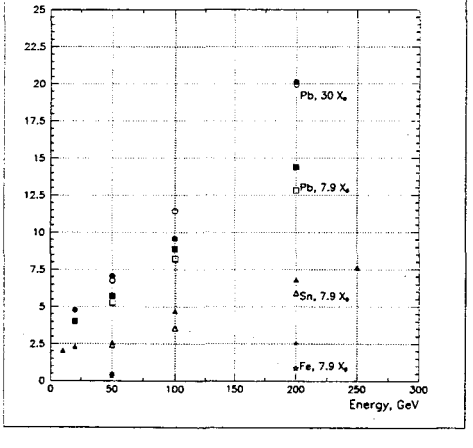

Figure 6. Backsplash (in percent) energy dependence for calorimeter placed at 45cm from ACD and threshold 0.3 MIP. Filled points are for test results, open points are for simulations. Circles - $30X_0$ lead calorimeter, squares - $7.9X_0$ lead, triangles - $7.9X_0$ tin, and stars - $7.9X_0$ iron

3.2. Energy dependence of backsplash. The measured backsplash energy dependence for different calorimeter materials is shown in Figure 6. This is given by filled points for tiles 6, 7, and 8 together (total area 432 cm^2), placed at 45 cm from the calorimeter face. The threshold used in this figure was 0.3 *mip*. The difference in the backsplash intensity between the iron and lead calorimeters, with the same thickness in radiation lengths, is quite dramatic. It is also seen that the backsplash is significantly lower for the $7.9X_0$ lead calorimeter than for $30X_0$ lead, especially at higher incident energy. This is due to the fact that the shower is not fully developed and contained in the thinner calorimeter at higher energy. Simulations results are also shown in Figure 6, by open points. The attempt to build the energy and threshold part of an empirical formula is demonstrated in Figure 7, where the energy fitting for the

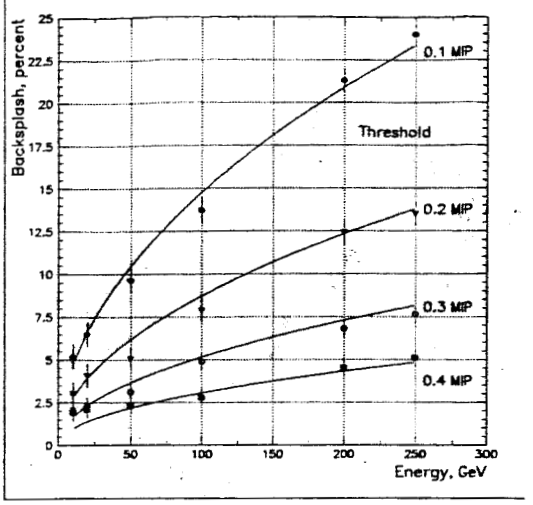

Figure 7. Fitting of backsplash energy dependence for 7.9X tin calorimeter at 45cm from ACD. Points represent test data, and lines – fitting.

tin calorimeter is given. The energy part of dependence is fitted by $E^{0.5}$, and the threshold dependence is fitted by $e^{-threshold/0.19mip}$. An average fitting precision of ~10% is achieved. It must be noted that this fitting is appropriate only for this material (Sn, or similar Z) and this thickness, appropriate for the GLAST ACD.

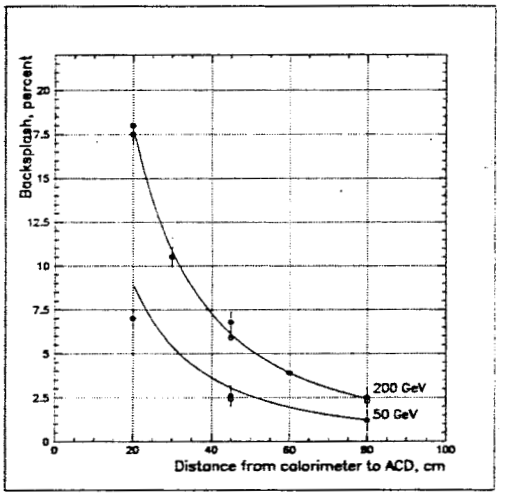

Figure 8. Backsplash distance dependence for $7.9X_0$ for two energies. Filled circles are for test data, open circles - simulations. Lines are for fitting by our formula

3.3 Backsplash distance dependence. Backsplash was measured for five different distances between the ACD and the calorimeter, using the tin calorimeter as the best imitator for a CsI calorimeter. Figure 8 shows the backsplash distance dependence for the $7.9X_0$ thick tin calorimeter. The data points are given by filled circles, and simulations results – by open circles, for energies 50 GeV and 200 GeV. The lines are the fittings by [55/(D+15)] where D is the distance between ACD and calorimeter front face in cm. For better fitting, the value 15, which is related to the position of the shower maximum in the calorimeter, should probably be energy dependent to reflect the shower development energy dependence. Combining all the effects we arrive at our empirical formula:

$$P_{backsplash} = 2.5 \times \exp\left(-\frac{E_{thr}}{0.19}\right) \times \frac{A}{432} \times \left(\frac{55}{D+15}\right)^2 \times \sqrt{E}$$

where $P_{backsplash}$ is the percentage probability of detecting backsplash, with threshold E_{thr} (measured in *mip*), in a tile of area A (in cm^2) separated by D cm from the front face of calorimeter, at an incident electron (photon) energy E (in GeV). This formula is valid for a calorimeter of $8\text{-}9X_0$ thick CsI (or material of similar average Z). The simulations and measurements agree within approximately 10%, which is acceptable for the present purposes.

Here we finished our efforts to build empirical formula for use in LAT ACD. Now we attempt to extend this formula to other calorimeter thicknesses and materials.

3.4 Calorimeter thickness dependence.

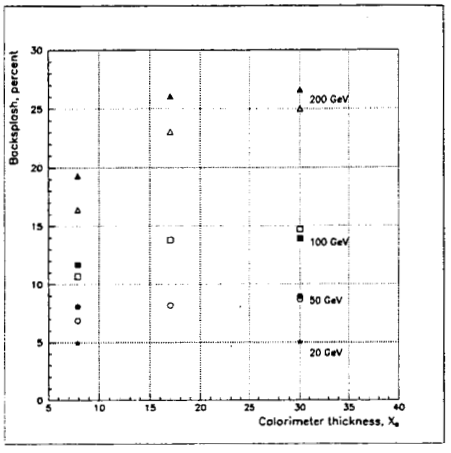

Figure 9. Backsplash thickness dependence for lead calorimeter placed at 45cm from ACD. Filled points are for test data, and open points - simulations. Triangles - 200 GeV, squares - 100 GeV, circles - 50GeV, and stars - 20 GeV

Measurements were performed for lead calorimeters of three thicknesses ($7.9X_0$, $17X_0$, and $30X_0$) and four incident energies (20, 50, 100, and 200 GeV). The results are shown in Figure 9. The increase in backsplash with increasing thickness from $7.9X_0$ to $17X_0$ and the saturation of the backsplash for $30X_0$ at these energies are due to the shower containment effect. (Shower maximum in lead is at ~$8.5X_0$ for 50 GeV, at ~$9X_0$ for 100 GeV, and at ~$9.7X_0$ for 200 GeV). Based on these results, we can slightly extend our formula for larger calorimeter thicknesses up to $13\text{-}14X_0$. A correction factor F to be applied to the backsplash value in our formula can be expressed as

$$F = 1 + 0.07\times (T\text{-}7.9),$$

where the calorimeter thickness in radiation lengths is T.

3.5 Calorimeter material dependence. It was noted in earlier simulations that backsplash intensity is strongly affected by the Z of the calorimeter material. Electromagnetic calorimeters of the same thickness in radiation lengths create less backsplash if they are made of lower Z (larger X_0 in g/cm^2) material. This can be explained by the fact that the backsplash consists mainly of soft photons whose attenuation is determined by grammage, not radiation lengths. Figure 10 shows the results of our test along with the simulations. These results demonstrate that, when the backsplash is an issue in the design of a high-energy electromagnetic calorimeter, it can be significantly reduced by optimizing the calorimeter material, but at the expense of increased calorimeter size and mass. We found that if the calorimeters have the same depth in radiation lengths, but are made of different

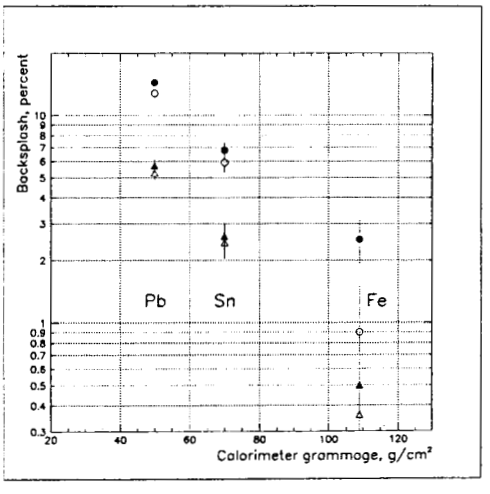

Figure 10. Backsplash for different calorimeter materials. Filled points are test data, and open circles - simulations. Circles are for 200 GeV, and triangles are for 50 GeV. Results are given for threshold of 0.3MIP, with calorimeters placed at 45cm from ACD

materials, the backsplash from them is proportional to $\approx Z^{1.95} e^{-0.04T}$, where Z is the calorimeter material atomic number and T is its depth in g/cm^2. These expressions can be used for qualitative consideration of the calorimeter material.

4. Predictions for GLAST ACD and Conclusions

We use the results obtained to check the GLAST ACD segmentation. The ACD was designed to the requirement that the backsplash-caused self-veto should remove not more than 20% of otherwise excepted gamma-ray events at 300 GeV, with a threshold in ACD set to 0.3 *mip*. This requirement is in conflict with the ACD charged particle detection efficiency requirement (to be >0.9997 over the entire ACD area), because higher detection efficiency can be achieved by reducing signal threshold, but that increases backsplash-caused self-veto. The backsplash prediction for GLAST ACD, based on our tests, is shown in Figure 11. It can be seen that at 300 GeV, self-veto due to backsplash is to be expected to be ~7% in the single ACD tile crossed by the incident gamma-ray, with the threshold set to 0.3 *mip*. This result is encouraging and provides some margin in ACD performance to meet the instrument requirements.

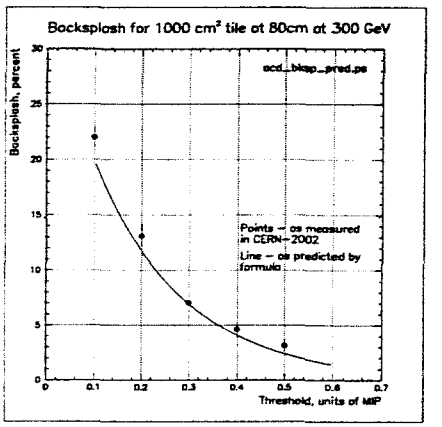

Figure 11. Predictions for LAT ACD for 1000 cm^2 tile at 80cm from calorimeter. Filled circles are data points as measured in test, scaled to the LAT ACD tile area. Line as predicted by our formula.

The empirical formula developed can be used in high-energy particle detector design where backsplash is an issue, avoiding complicated and time-consuming Monte Carlo simulations. The results obtained also can be used in calorimeter optimization, for example in the proposed ACCESS mission for detection of high-energy cosmic rays, where the backsplash is also an undesirable effect.

5. Acknowledgements

This work could not have been completed without the extremely valuable help of Deneen Ferro and Bill Daniels (detector fabrication and refurbishing) and Norm Dobson (data acquisition system). The authors are very grateful to Prof. Tune Kamae and Tsunefumi Mizuno for their help in conducting the beam test and to Steven Ritz for very valuable discussions and recommendations in the preparation stage. Special thanks go to CERN SPS personnel, who were extremely helpful in all aspects of the beam test.

6. References

1. Fichtel, C.E. et al. ApJ, 198, 163, 1975

2. Bennett, K. Nuclear Physics B (Proc. Suppl) 14B (1990) 23-34.

3. Thompson, D.J. et al. Astrophysical Journal, 86, 629, 1993

4. Fichtel, C.E. et al. Astronomy & Astrophysics Suppl. Ser. 97, 13, 1993,

5. Akimov et al. 1991, Astronomicheskiy Zhurnal, 17, #6, pp.501-504.

6. Gehrels, N., and Michelson, P. Astroparticle Phys. 11, 277, 1999